Self-Focusing of Optical Beams

R. Y. Chiao[1], T. K. Gustafson[2], and P. L. Kelley[3]

[1] School of Engineering, University of California, Merced, California, USA
rchiao@ucmerced.edu
[2] Department of Electrical Engineering and Computer Science, University of California, Berkeley, California, USA
tkg@eecs.berkeley.edu
[3] Department of Electrical and Computer Engineering, Tufts University, Medford, Massachusetts, USA
pkelley@tufts.edu

1 Abstract

The nonlinear index of refraction is responsible for many effects in optical beam propagation, including self-focusing. We will review self-focusing and related phenomena and discuss physical mechanisms which give rise to the refractive index nonlinearity.

2 Introduction

Optical self-action effects occur when an electromagnetic field induces a refractive index change in the medium through which the field propagates. The change in index then exhibits a back-action on the field so as to influence its propagation characteristics. The principal effects are shown in the following table.

	Spatial	Temporal
Instabilities	Light-by-Light Scattering	Modulational Instability
Envelope Effects	Spatial self-phase modulation	Temporal self-phase modulation - self-chirping
	Self-focusing - whole-beam and multimode	Self-Compression Self-decompression - self-dispersion Self-steepening
	Self-trapping - spatial solitons	Temporal solitons
Combined	Light Bullets	

The consequences of these nonlinear effects can be significant. In beam propagation, self-focusing and self trapping lead to lowering of thresholds for other nonlinear

processes, such as stimulated Raman and Brillouin scattering, self-phase modulation, and optical damage. Nonlinear index effects impact the design of very high energy laser systems such as those required for laser fusion and the implementation of long distance fiber optical communication systems.

3 Early history

Two years after self-focusing in plasmas was proposed in 1962 [1], the theory of self-trapping was developed [2, 3]. In reference [2], a numerical solution was given for a two transverse dimension beam, the critical power was calculated, mechanisms for the nonlinearity were discussed, and the effect was used to explain anomalous Raman gain and optical damage. In both 1964 references the one-transverse-dimension hyperbolic secant soliton solution was given. The theory of self-focusing was developed in 1965 [4, 5]. Reference [5] estimates the self-focusing distance, derives the nonlinear Schrödinger equation (NLSE), and uses this equation to obtain numerical results on self-focusing. That same year the first observation of self-focusing was made [6] and it was experimentally related to anomalous stimulated Raman gain [7, 8]. In 1966, the theory of nonlinear instability was given [9, 10] and the effect observed experimentally [11]. In this same year, multifilament structure in multimode beams was observed and the influence on spectral broadening was considered [12]; this was followed several years later by experiments in which regular filament structure was seen on carefully prepared beams [13].

Since this initial work a number of important contributions have been made. As of 2006, when this article was written, there were about 1000 papers with self-focusing in the title and more than 500 papers with self-trapping or spatial solitons in the title. The early work on self-focusing has been reviewed [14, 15, 16, 17] and considerable attention has been given to mathematical methods for dealing with blow-up of solutions to the NLSE and related equations in physics (see references [18] and [19] for a discussion of these problems). Modification of self-focusing theory due to the finite duration of pulses has also been considered [20, 21, 22, 23, 24, 25]. For a recent source of references on self-focusing and self-trapping, see [26]. A unified approach to self-action effects is given in [27].

In our review, we take an approach which is opposite to much of the historical sequence. We will first discuss instabilities, then beam self-focusing, and finally self-trapping.

4 Nonlinear polarization and the nonlinear refractive index

Self-action effects arise from the third order nonlinear polarization. Slow molecular motions can contribute to the nonlinear response because the nonlinear polarization includes terms for which the slowly varying part of the square of the field amplitude drives the material system. This can lead to very strong nonlinearities.

In most cases, the refractive index increases with increasing light intensity. A very simple example occurs for ensembles of anisotropic molecules. Since the molecules have lowest energy when they are aligned in the direction(s) of highest polarizability, they experience a torque that increases the fractional alignment and the index of refraction. Increasing density of an initially uniform fluid in the region of the beam (electrostriction) or moving molecules of higher polarizability than a surrounding fluid into a beam also lowers the energy and results in a positive nonlinear refractive index.

Neglecting dispersion, the polarization can be written,

$$P = \varepsilon_0 \chi E \tag{1}$$

where E is the electric field, and χ is the electric susceptibility including nonlinear terms. For simplicity, we assume the various frequency and wavevector components of the field are all polarized in the same direction. We write the susceptibility

$$\chi = \chi^{(1)} + \chi^{(3)} \langle E^2 \rangle, \tag{2}$$

where $\langle E^2 \rangle$ is the average of E^2 over a few optical cycles. We have assumed there are no contributions to the polarization in even powers of the field and have neglected any contributions by odd powers beyond the third order term. We can replace $\chi^{(1)}$ and $\chi^{(3)}$ by the linear and nonlinear refractive index, n_0 and n_2, where

$$n = n_0 + 2 n_2 \langle E^2 \rangle, \tag{3}$$

The linear refractive index is given by

$$n_0 = \sqrt{1 + \chi^{(1)}} \tag{4}$$

while the nonlinear refractive index is given by

$$n_2 = \frac{\chi^{(3)}}{4 n_0}, \tag{5}$$

assuming the nonlinear term is much smaller than the linear term. We can then write the polarization as

$$P = P^{\text{L}} + P^{\text{NL}} \tag{6}$$

where

$$P^{\text{L}} = \varepsilon_0 (n_0^2 - 1) E \tag{7}$$

and

$$P^{\text{NL}} = 4 \varepsilon_0 n_0 n_2 \langle E^2 \rangle E. \tag{8}$$

Eqn. 8 is the induced polarization to third power in the electric field. We have neglected polarization terms that occur at the sum of three optical frequencies and have kept terms that are close to at least one of the driving frequencies. This neglect of "third harmonic" terms can be justified by assuming they are small or not phase matched. However, we do not assume contributions due to material resonances at the sum of two driving frequencies are negligible; these terms do contribute to n_2.

5 The non-linear Schrödinger equation

To facilitate our understanding of the self-focusing problem we use an approximation to the scalar nonlinear wave equation which has the familiar form of a Schrödinger equation [5]. We assume a single frequency and use the slowly varying amplitude approximation. We first write the field in terms of its positive and negative frequency components

$$E = \tfrac{1}{2}(E^+ + E^-), \tag{9}$$

where $E^- = E^{+*}$. The positive frequency component is given by

$$E^+(\mathbf{r}, t) = \mathcal{E}(\mathbf{r})\, e^{i(kz-\omega t)} \tag{10}$$

where $k = \omega n_0(\omega)/c$ and we have assumed the wave is traveling in the $+z$ direction. In the slowly varying amplitude approximation, it is assumed that $\left|\partial^2\mathcal{E}/\partial z^2\right| \ll k\left|\partial\mathcal{E}/\partial z\right|$. This leads to the following approximation to the wave equation

$$i\frac{\partial\mathcal{E}}{\partial z} + \frac{1}{2k}\nabla_\perp^2\mathcal{E} + k\frac{n_2}{n_0}\left|\mathcal{E}\right|^2\mathcal{E} = 0. \tag{11}$$

6 Four-wave mixing, weak-wave retardation, instability

In this section, we discuss the coupling of waves through the nonlinear index. This will lead to a discussion of spatial instabilities in monochromatic plane waves. From a Fourier component point of view, the nonlinear interaction involves the coupling of three field components to produce a nonlinear polarization which drives a fourth field component. The basic process can be described as light-by-light scattering four-wave mixing.

We separate the field into weak and strong parts. This is convenient as it allows us to linearize the problem in the weak field. It is appropriate when a strong optical beam from a laser initially enters the nonlinear medium and the weak field is assumed to be much smaller than the strong field. In fact, the initial weak field can be the zero point field so that the weak wave is initiated by spontaneous emission. We can write

$$\mathcal{E} = \mathcal{E}_s + \mathcal{E}_w, \tag{12}$$

where *s* and *w* stand for strong and weak, respectively. Neglecting terms in the weak field beyond the linear term we have for the strong field nonlinear polarization.

$$\mathcal{P}_s^{\text{NL}} = 2\varepsilon_0 n_0 n_2 \left|\mathcal{E}_s\right|^2 \mathcal{E}_s \tag{13}$$

and for the weak field nonlinear polarization

$$\mathcal{P}_w^{\text{NL}} = 2\varepsilon_0 n_0 n_2 \left(2\left|\mathcal{E}_s\right|^2 \mathcal{E}_w + \mathcal{E}_s^2\mathcal{E}_w^*\right) \tag{14}$$

This result has two interesting aspects. First, the weak wave experiences twice the nonlinear polarization and index of refraction change (the first term in Eqn. 14) as the

strong field induces on itself (Eqn. 13). The weak wave retardation can compensate for the breaking of phase matching by diffraction [10]. Second, the positive and negative parts of the weak field are coupled to each other (the second term in Eqn. 14). Because of the cross coupling, phase conjugation occurs and coupled frequency and propagation vector sidebands grow on the strong field.

To calculate the instability gain, we assume a strong plane-wave together with two weak components traveling very nearly parallel to the strong wave as shown in Fig. 1. The weak-wave retardation effect is also shown in the figure.

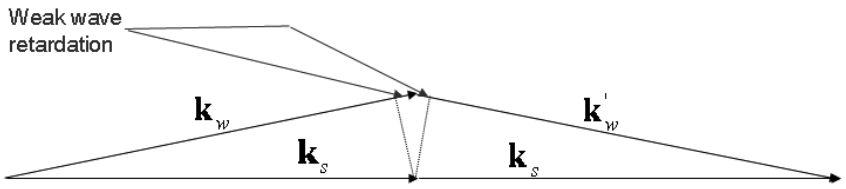

Fig. 1. Light-by-light scattering. Strong forward wave ($\mathbf{k}_s$) interacting with two weak waves ($\mathbf{k}_w, \mathbf{k'}_w$) whose magnitudes are increased by weak-wave retardation.

From the NLSE (Eqn. 11) the exponential growth and decay constants for the weak-wave power are found to be[9]

$$g = \pm k_\perp \left(\frac{4n_2}{n_0} \left| \mathcal{E}_s \right|^2 - \frac{k_\perp^2}{k^2} \right)^{1/2} \tag{15}$$

where $k_\perp$ is the component of the scattered wave that is perpendicular to the strong wave. Since $k_\perp \ll k$, for all the cases of interest, $k_\perp$ can be replaced by $k\theta$ where θ is the angle between the strong wave and the weak waves. A plot of g vs. θ is given in Fig. 2. Note that the maximum value of g is $g_{\max} = 2kn_2 \left| \mathcal{E}_s \right|^2 / n_0$ and the angle at which this occurs is $\theta_{\text{opt}} = 2\sqrt{2n_2} \left| \mathcal{E}_s \right|^2 / n_0$. Because of the cross-coupling, the normal Fourier components of the scattered waves grow (or decay) in pairs, one at θ and the other at $-\theta$. As we shall see from the discussion of self-focusing given below, the instability gain is related to the beam self-focusing distance.

An example of light-by-light scattering is shown in Fig. 2. A strong forward beam is sent into a short cell containing nitrobenzene, a medium with large n_2. To obtain the strong beam, a Q-switched ruby laser with 240 MW power was focused to an area of 20 mm^2. This is the central peak in the figure. When a weak beam was sent in at an angle $+\theta$ to the strong beam, a second weak beam at $-\theta$ appeared.

7 Spatial self-phase modulation and estimating the beam self-focusing distance

In order to understand the nonlinear propagation of spatially finite beams, we first consider the effect on a beam of the nonlinear polarization alone. If diffraction is neglected

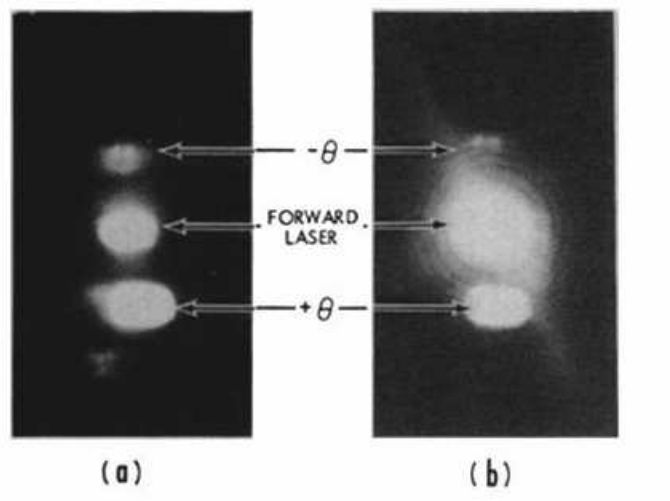

Fig. 2. (a) Typical data for a 3 mm cell length where no self-focusing occurs. Due to overexposure, the actual intensity ratios are not faithfully reproduced. (b) Simultaneous 1.5 cm spacer Fabry-Perot interferometer analysis of all three beams from the 3 mm cell.

in the wave equation, Eqn. 11, the solution for the nonlinear phase build-up from an input boundary at $z = 0$ is

$$\Phi_{\text{NL}}(\mathbf{r}, z) = kz\frac{n_2}{n_0}|\mathcal{E}(\mathbf{r}, 0)|^2 \tag{16}$$

where $\mathbf{r}$ is the coordinate vector transverse to z. We can define the nonlinear distance by setting the phase deviation across the beam $\Delta\Phi_{\text{NL}}$ equal to 1, so that

$$z_{\text{NL}} = \frac{n_0}{kn_2|\mathcal{E}(0,0)|^2} = \frac{2}{g_{\max}} \tag{17}$$

From the wave equation we see that there is also a characteristic distance for diffraction. We take this to be

$$z_{\text{DIF}} = kr_0{}^2 \tag{18}$$

where r_0 is a distance characteristic of the beam radius. Note that z_{DIF} is the Rayleigh range or the Fresnel length of the beam.

The transverse component of the wave-vector at a transverse point $\mathbf{r}$ in a beam is

$$\mathbf{k}_\perp(\mathbf{r}, z) = \nabla_\perp\Phi_{\text{NL}}(\mathbf{r}, z) = kz\frac{n_2}{n_0}\nabla_\perp|\mathcal{E}(\mathbf{r}, 0)|^2 \tag{19}$$

The variation of $\mathbf{k}_\perp$ with $\mathbf{r}$ can be viewed as a spatial chirp. A plot of $k_\perp$ is shown in Fig. 3

For a beam that is symmetric with either circular or slab symmetry, the angle the wave-vector makes with the z-axis for small angles is

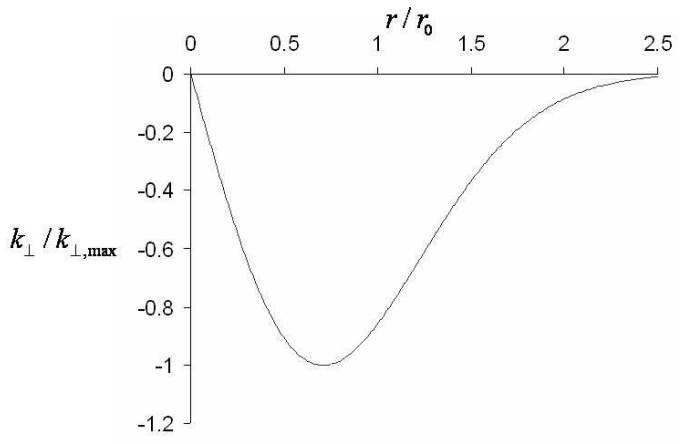

Fig. 3. $k_\perp$ versus r for a Gaussian beam. r_0 is the 1/e intensity half-width and $k_{\perp,\max} = -kzn_2|\mathcal{E}(0,0)|^2\sqrt{2}e^{\frac{1}{2}}/n_0 r_0$. Near $r = 0$, the spatial chirp is linear as it is for a conventional lens.

$$\theta(r,z) = z\frac{n_2}{n_0}\frac{\partial|\mathcal{E}(r,0)|^2}{\partial r} \tag{20}$$

a result which is independent of wavelength. Assuming the beam is most intense at the center, θ is negative and the beam will focus when we include the diffraction term. An estimate of the focusing distance can be found by setting $\theta(r,z) = r/z$, the angle that a ray starting at r will reach the beam axis at z. When $z_{\text{DIF}} \gg z_{\text{NL}}$ this gives a self-focusing distance [5]

$$z_{\text{SF}} = \sqrt{\frac{-n_0 r}{n_2\partial|\mathcal{E}|^2/\partial r}}\Bigg|_{r\to 0} \tag{21}$$

Assuming a Gaussian beam with r_0 equal to the intensity 1/e halfwidth and using Eqs. 17 and 18, we find

$$z_{\text{SF}} = \sqrt{\frac{z_{\text{NL}}z_{\text{DIF}}}{2}}. \tag{22}$$

A similar result for the self-focusing distance can be found by simply inserting the angle corresponding to the Fourier inverse of the beam radius into Eq. 15 for the instability gain.

8 Self-focusing intensity singularity and beam collapse

If a beam is has circular symmetry, it will nonlinearly focus without limit to an intensity singularity. On the other hand, slab beams that are confined in only one transverse

dimension will not focus to a singularity. This difference between one and two dimensional focusing is easy to understand by simple scaling arguments. From the NLSE, Eqn. 11, we see that in both cases the diffraction term scales as the inverse of the beam width squared. In the two dimensional transverse confinement case, the nonlinear term also scales as the reciprocal of the beamwidth squared since this term is proportional to intensity and power is conserved. Because the scaling of the two terms is the same, the dominant term will remain dominant and in this situation the beam will come to a catastrophic focus when the nonlinear term dominates.

For confinement in one transverse dimension, the nonlinear term scales as the inverse of the beamwidth because the power per unit distance in the unconfined direction is conserved. Since the nonlinear term is only proportional to the inverse first power of the beamwidth, the nonlinear term will grow more slowly with decreasing radius than the diffraction term. The diffraction term comes into balance with the focusing term and there is self focusing without an intensity singularity.

We will examine the two-transverse-dimensions case in further detail. Although there are a number of ways to analyze the problem, we will numerically solve the NLSE for cylindrical symmetry using a finite difference method. In reference [5], the finite difference solution involved directly calculating the transverse derivatives. Here we will use the split-step method where the transverse diffraction term in the NLSE is calculated in Fourier space and the nonlinear term in the NLSE is calculated in coordinate space. To efficiently solve the cylindrically symmetric problem we use a version of the fast Hankel transform given in reference [28]. The method can be used to come close to the initial singularity in a very computationally efficient fashion. With the split-step method we can also avoid the paraxial approximation by using the nonlinear Helmholtz equation to directly calculate the contribution of the transverse diffraction term to the axial phase factor in Fourier space.

The result of a typical calculation for an initially Gaussian beam is shown as the outer curve in Fig. 4. The estimated self-focusing distance, as given by Eqn. 21, is found to be smaller than the numerically calculated distance in part because the estimated distance does not take into account the effect of diffraction in lengthening the self-focusing distance. Comparing the present split-step Hankel with the early calculation [5], there is a least order of magnitude decrease in computation time and about a factor of one hundred increase in intensity near the focus. This improvement can be attributed to both the efficiency of the present algorithm and the increase in computer speed.

In addition to the intensity singularity, it is possible to show that beams undergoing self-focusing collapse in the NLSE approximation. Collapse occurs when the entire beam shrinks to a point. Reference [29] obtained a second order differential equation for the RMS beam radius which in the two-transverse-dimension case can be written in terms of the ratio of two invariants. Because of the Schrödinger character of Eqn. 11, the two invariants correspond to the expectation value of the Hamiltonian and the expectation value of the unnormalized probability density. In the cylindrically symmetric case, the equation for the average beam radius is:

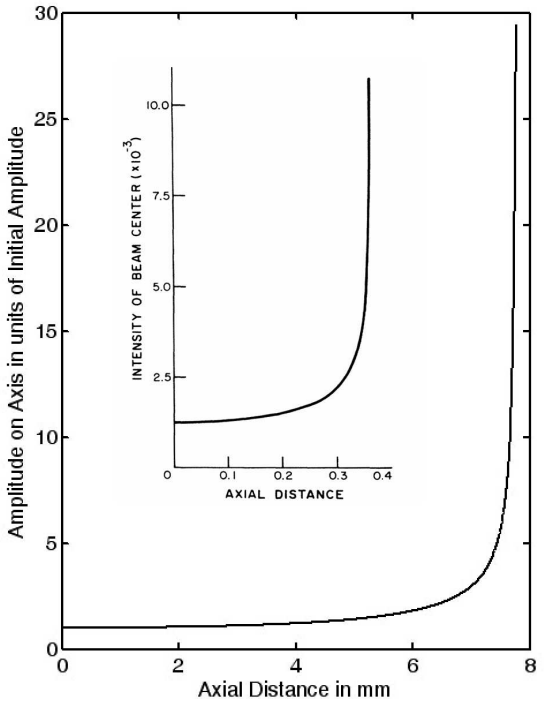

Fig. 4. Numerical calculations of the approach to the self-focus. For the outer curve, the self-focusing distance is found to be ≈ 7.8 mm. The initially Gaussian beam at $\lambda = 1$ μm with $r_0 = 70.7$ mm has $z_{\text{DIF}} = 31.4$ mm, $z_{\text{NL}} = 3.14$ mm, and from Eqn. 21 $z_{\text{SF}} = 7.02$ mm. The inset shows an early numerical calculation of self-focusing [5].

$$\frac{d\left\langle r^2\right\rangle}{dz^2} = 2\frac{\int\left(\frac{1}{k^2}\left|\nabla_\perp\mathcal{E}\right|^2 - \frac{2n_2}{n_0}\left|\mathcal{E}\right|^4\right) rdr\Big|_{z=0}}{\int\left|\mathcal{E}\right|^2 rdr\Big|_{z=0}}, \tag{23}$$

where the numerator is the Hamiltonian term and the denominator is the unnormalized probability density. On carrying out the integrations for an initially Gaussian beam we find,

$$\langle r(z)^2\rangle = r_0^2 + \left(\frac{1}{k^2 r_0^2} - \frac{n_2|\mathcal{E}(0,0)|^2}{2n_0}\right) z^2. \tag{24}$$

When $n_2|\mathcal{E}(0,0)|^2/2n_0 > 1/k^2 r_0^2$ the beam will collapse. From this equation, we can obtain the collapse distance

$$z_{\text{COL}} = \sqrt{\frac{2z_{\text{NL}} z_{\text{DIF}}}{1 - \frac{2z_{\text{NL}}}{z_{\text{DIF}}}}} \tag{25}$$

When $z_{\rm DIF} \gg z_{\rm NL}$, we find that $z_{\rm COL} = \sqrt{2 z_{\rm NL} z_{\rm DIF}}$, a factor of 2 greater than the self-focusing distance given in Eqn. 22. For the case of Fig. 4, where $z_{\rm DIF} = 31.4$ and $z_{\rm NL} = 3.14$, we find from Eqn. 25 that $z_{\rm COL} = 15.7$ which is also about a factor of two larger than the distance where blow-up is observed in the numerical calculation.

9 Limitations on blow-up and collapse

It should be apparent that much of the analysis given here is of mathematical significance rather than representing actual physics since the NLSE involves several limitations, including the use of the scalar wave equation, the slowly varying amplitude assumption, the absence of saturation of the nonlinear index, and the neglect of other nonlinearities. These nonlinearities include stimulated light scattering, optical damage, and breakdown. That these other nonlinear effects become important is evidenced by the orders of magnitude increase in intensity due to self-focusing as shown, for example, in Fig. 4. In addition, beams with small scale structure exhibit a complex breakup process as discussed in the next section.

The stabilization of self-focusing resulting in self-trapping requires consideration of processes not included in the simple expression (Eqn. 3) for the nonlinear dielectric response. For liquids, observed focal spots can vary from a few microns in size to a few tens of microns depending upon the liquid. The stabilizing process either limits the nonlinear increase in the index of refraction or depletes the forward beam in a strongly nonlinear fashion. The former includes saturation of the nonlinear index [30, 31, 32] and the latter stimulated light scattering [33] or a negative contribution to the index due to the production of electrons on ionization of the liquid in the intense light field [34].

In air, in particular, the critical power is approximately 2 GW for a diffraction limited Gaussian beam [35]. When the intensity approaches 10^{13} to 10^{14} W/cm^2, multiphoton ionization occurs. The resultant intensity dependent reduction of the refractive index arising from the consequent underdense plasma can stabilize the beam. Thin intense filaments over tens (and up to hundreds) of meters has been observed. A theoretical description has been given by generalizing Eqn. 11 to include both ionization and a Kerr effect which has both a non-dispersive and a dispersive contribution [36].

An understanding and control of the nonlinear optical interaction resulting in self-focussing and self-trapping as well as the associated phenomena in the Table has resulted in the ability to nonlinearly shape optical beams in a controlled manner.

10 Beam breakup and multiple filament formation

Small scale beam structure can play an important role in self-focusing [12, 13]. Fig. 5 shows small scale filament formation during self focusing of a beam. This effect is particularly significant when the beams have structure at angles near $\theta_{\rm opt}$. For most beams where self-focusing is significant, $\theta_{\rm opt} \gg \theta_{\rm av} = 1/kr_0$ so that $g_{\rm max} z_{\rm SF} \gg 1$. It then becomes a question of whether a beam is sufficiently smooth initially that whole beam

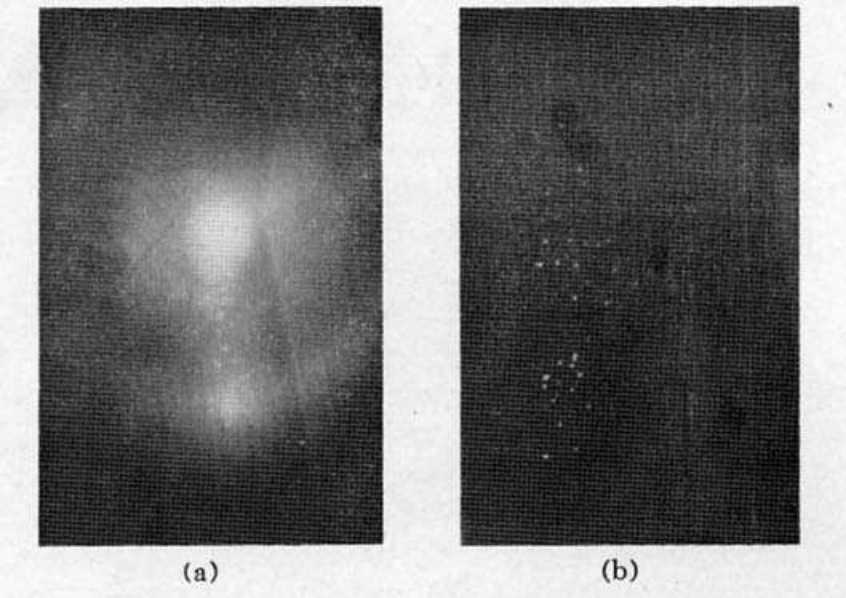

Fig. 5. (a) Image of a laser beam emerging from a 50-cm cell of CS_2 and exhibiting large- and small-scale trapping. Magnification is 30x. The bright central portion is the large-scale trapped beam; the many small bright filaments demonstrate the small-scale trapping. The broad disk and ring of light are the untrapped beam diffracting from the initial pinhole. (b) Raman Stokes radiation under conditions similar to (a). Magnification 50x. From [12].

focusing can dominate beam breakup into multiple small scale filaments. To further understand this, we return to the instability analysis discussed earlier. Figure 6 gives a rough schematic of the different contributions to the self-focusing of a typical beam: the small box on the left includes the angular region corresponding to the transverse Fourier components for a smooth beam, the middle box encompasses the region where beam fine structure contributes, and the right box corresponds to Fourier components that must grow from noise including zero point oscillations. The height of each box corresponds to the typical gain in each of the three regions. Increasing gain with angle is offset by decreasing initial Fourier amplitude.

11 Self-focusing of pulses - light bullets

When an optical pulse transverses the nonlinear medium, the focusing distance becomes time dependent as well as radially dependent. The most obvious consequence of this is that the most intense portions are focused at a shorter distance than the weaker leading and trailing edges. References [20] and [21] first considered the motion of the focal regions for temporal pulses. Reference [22] included retardation and theoretically deduced the trajectories of the moving focal regions for a Gaussian temporal amplitude

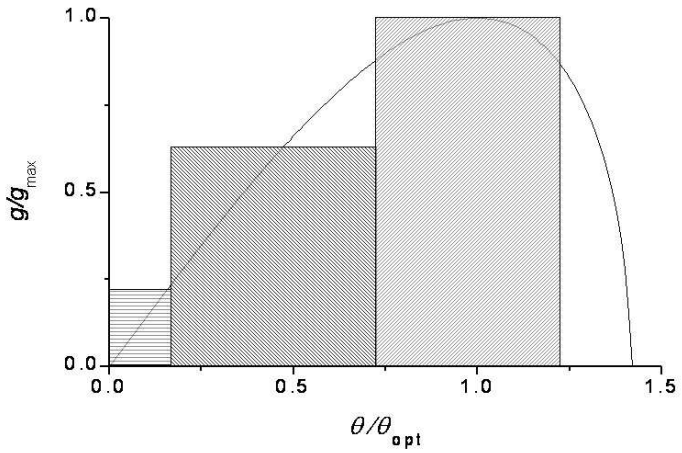

Fig. 6. Weak-wave gain, g, versus angle, θ, between the weak and strong waves as calculated from Eqn. 15. The contributions of the three shaded regions are described in the text.

profile with a 1/e halfwidth of t_p at the entrance boundary. Due to the retardation, the distance at which the focal region first appears exceeds z_{SF}, the focussing distance for the peak of the pulse. This emanates from a portion of the pulse shifted to the leading edge by an amount dependent upon the initial pulse width. This shift is $t_p(ct_p/2n_0z_{\text{SF}})$ for a pulse whose length t_p/n_0 is much less than z_{SF}. For such a pulse the initial focussing distance exceeds z_{SF} by a distance equal to $[(c/n_0t_p)^2/4z_{\text{SF}}]$. The focal region subsequently expands forward, and also expands backwards to the minimum focussing distance, z_{SF}, at time $z_{\text{SF}}n_0/c$ corresponding to the peak. Subsequently the focal region continues to expand as it propagates through the medium. The details of this time dependent behavior has been investigated both experimentally [23, 24] and theoretically [25].

When anomalous group velocity dispersion is included in the NLSE then a balance can occur between the dispersion and the phase buildup due to the nonlinearity and a three dimensional trapped pulse - or "light bullet" can propagate [37] . There has been an extensive investigation of such temporally and spatially trapped light .

12 Self-trapping, spatial solitons

If a beam has circular symmetry it will focus to an intense singularity. When $z_{\text{DIF}} \approx z_{\text{NL}}$, a solution to the wave equation for a beam can be found whose transverse intensity profile does not vary in z. Since both of these parameters (z_{DIF} and z_{NL}) are proportional to the reciprocal of the radius, the self-trapped solution in two transverse dimensions occurs at a critical power independent of the beam radius. Using the values of z_{NL} and

z_{DIF} given in Eqs. 17 and 18 the critical power can be estimated by setting these two characteristic parameters equal obtaining

$$P_{\text{CR}} = \frac{n_0 c \lambda^2}{8\pi n_2} \tag{26}$$

This can be compared with numerical results [2].

In case of confinement in one transverse direction, the following constraint applies

$$\frac{dP}{dy} r_0 \approx \frac{\varepsilon_0 c \lambda^2}{(2\pi)^2 n_2} \tag{27}$$

where dP/dy is the power per unit distance in the transverse direction perpendicular to the confinement direction. In this case, there is no critical power per unit distance. Whatever value dP/dy of one chooses there is an r_0 such that Eqn. 27 is satisfied. The lowest order hyperbolic secant solution has been known since 1964 [2, 3], and inverse scattering theory has been used to find higher order analytic solutions [38].

References

1. G . A. Askar'yan. Effects of the gradient of a strong electromagnetic beam on electrons and atoms. *JETP*, 15:1088–1090, 1962.
2. R.Y. Chaio, E. M. Garmire, and C. H. Townes. Self-trapping of optical beams. *Phys. Rev. Lett.*, 13:479–482, 1964. Erratum, ibid, 14:1056, 1965.
3. V. I. Talanov. Self-focusing of electromagnetic waves in nonlinear media. *Radiophys.*, 8:254–257, 1964.
4. V. I. Talanov. Self-focusing of wave beams in nonlinear media. *Radiophys.*, 9:138–141, 1965.
5. P. L. Kelley. Self-focusing of optical beams. *Phys. Rev. Lett.*, 15:1005–1008, 1965.
6. N. F. Pilipetskii and A. R. Rustamov. Observation of self-focusing of light in liquids. *JETP Lett.*, 2:55–56, 1965.
7. Y. R. Shen and Y. J. Shaham. Beam deterioration and stimulated raman effect. *Phys. Rev. Lett.*, 15:1008–1010, 1965.
8. P. Lallemand and N. Bloembergen. Self-focusing of laser beams and stimulated raman gain in liquids. *Phys. Rev. Lett.*, 15:1010–1012, 1965.
9. V.I. Bespalov and V. I. Talanov. Filamentary structure of light beams in nonlinear liquids. *JETP Lett.*, 3:307–309, 1966.
10. R. Y. Chiao, P. L. Kelley, and E. M. Garmire. Stimulated four-photon interaction and its influence on stimulated rayleigh-wing scattering. *Phys. Rev. Lett.*, 17:1158–1161, 1966.
11. R. L. Carman, R. Y. Chiao, and P. L. Kelley. Observation of degenerate stimulated four-photon interaction and four-wave parametric amplification. *Phys. Rev. Lett.*, 17:1281–1283, 1966.
12. R. Y. Chiao, M. A. Johnson, S. Krinsky, H. A. Smith, C. H. Townes, and E. M. Garmire. A new class of trapped light filaments. *IEEE J. Quantum Electron.*, QE-2:467–469, 1966.
13. A. J. Campillo, S. L. Shapiro, and B. R. Suydam. Periodic breakup of optical beams due to self-focusing. *Appl. Phys. Lett.*, 23:628–630, 1973.
14. S. A. Akhmanov, R.V. Khokhlov, and A. P. Sukhorukov. in *Laser Handbook* F. T. Arecchi and E.O. Shulz-Dubois, eds. (Elsevier, New York, 1972), Vol. 2 pp 1151.

15. O. Svelto. in *Progress in Optics* Vol. XII edited by E. Wolf (North Holland, Amsterdam, 1974), p 35.
16. Y. R. Shen. Self-focusing: Experimental. *Prog. Quant. Electron.*, 4:1–34, 1975.
17. J. H. Marburger. Self-focusing: Theory. *Prog. Quant. Electron.*, 4:35–110, 1975.
18. J. J. Rasmussen and K. Rypdal. Blow-up in nonlinear Schrödinger equations - I A general review. *Physica Scripta*, 33:481–497, 1986.
19. K. Rypdal and J. J. Rasmussen. Blow-up in nonlinear Schrödinger equations - II Similarity structure of the blow-up singularity. *Physica Scripta*, 33:498–504, 1986.
20. A. L. Dyshko, V. N. Lugovoi, and A. M. Prokhorov. Self-focusing of intense light beams. *JETP Lett.*, 6:146–148, 1967.
21. V. N. Lugovoi and A. M. Prokhorov. A possible explanation of the small scale self-focusing light filaments. *JETP Lett.*, 7:117–119, 1968.
22. J.-P. E. Taran and T. K. Gustafson. Comments on the self-focusing of short light pulses. *IEEE Journal of Quantum Electronics*, 5:381–382, 1968.
23. M. M. T. Loy and Y. R. Shen. Small scale filaments in liquids and tracks of moving foci. *Phys. Rev. Lett.*, 22:994–997, 1969.
24. M. M. T. Loy and Y. R. Shen. Experimental study of small-scale filaments of light in liquids. *Phys. Rev. Lett.*, 25:1333–1336, 1970.
25. Y. R. Shen and M. M. T. Loy. Theoretical interpretation of small-scale filaments originating from moving focal spots. *Phys. Rev. A*, 3:2099–2105, 1971.
26. Y. S. Kivshar and G. P. Agrawal. *Optical Solitons*. Academic Press, Boston, 2003.
27. P. L. Kelley. Nonlinear index of refraction and self-action effects in optical propagation. *IEEE Sel. Top. Quant. Electron.*, 6:1259–1264, 2000.
28. M. Guizar-Sicairos and J. C. Gutierrez-Vega. Computation of quasi-discrete Hankel transforms of integer order for propagating optical wave fields. *J. Opt. Soc. Am.*, A21:53–58, 2004.
29. S. N. Vlasov, V. A. Petrishchev, and V. I. Talanov. Averaged description of wave beams in linear and nonlinear media (the method of moments). *Quantum Electron. Radiophys.*, 14:1062–1070, 1971.
30. T. K. Gustafson, P. L. Kelley, R.Y. Chiao, R. G. Brewer, and C. H. Townes. Self-trapping of optical beams. *Appl. Phys. Lett.*, 12:165–168, 1968.
31. J. Marburger, L. Huff, J.D. Reichert, and W. G. Wagner. *Phys. Rev.*, 184:255–259, 1969.
32. T. K. Gustafson and C. H. Townes. *Phys. Rev. A*, 6:1659–1664, 1972.
33. P. L. Kelley and T. K. Gustafson. Backward stimulated light scattering and the limiting diameters of self-focused light beams. *Phys. Rev. A*, 8:315–318, 1973.
34. E. Yablonovitch and N. Bloembergen. *Phys. Rev. Lett.*, 29:907–910, 1972.
35. J. Kasparian, R. Sauerbrey, and S. L. Chin. The critical laser intensity of self-guided light filaments in air. *Appl. Phys. B*, 71:877–879, 2000.
36. A. Couairon and L Berge. Light filaments in air for ultrviolet and infrared wavelengths. *Phys. Rev. Lett.*, 71:35003 1–4, 2002.
37. Y. Silberberg. Collapse of optical pulses. *Optics Letters*, 15:1282–1284, 1990.
38. V. E. Zakharov and A. B. Shabat. Exact theory of two-dimensional self-focusing and one-dimensional self-modulation of waves in nonlinear media. *JETP*, 34:62–69, 1972.